TETRAHEDRAL SYMMETRY in ATOMIC NUCLEI

Y.S. Chen
China Institute of Atomic Energy,
Presentation at TPI, 8 June, 2012.

1. Introduction
2. Brief description of RASM
3. Tetrahedral symmetry in SHE
4. Remarks

Introduction

Tetrahedral symmetry

The tetrahedral symmetry is quite common in molecular, metallic clusters, and some other quantum objects.

The tetrahedral symmetry is a direct consequence of the point group and corresponds to the invariance under transformation of the group T_d^D ,which has two one- and one four-dimensional irreducible representation.

The double point group T_d^D leads to 'exotic' fourfold degeneracies of single particle levels. This high degeneracy aspect leads to high stability of implied nuclear shape.

C4 Tetrahedral symmetry

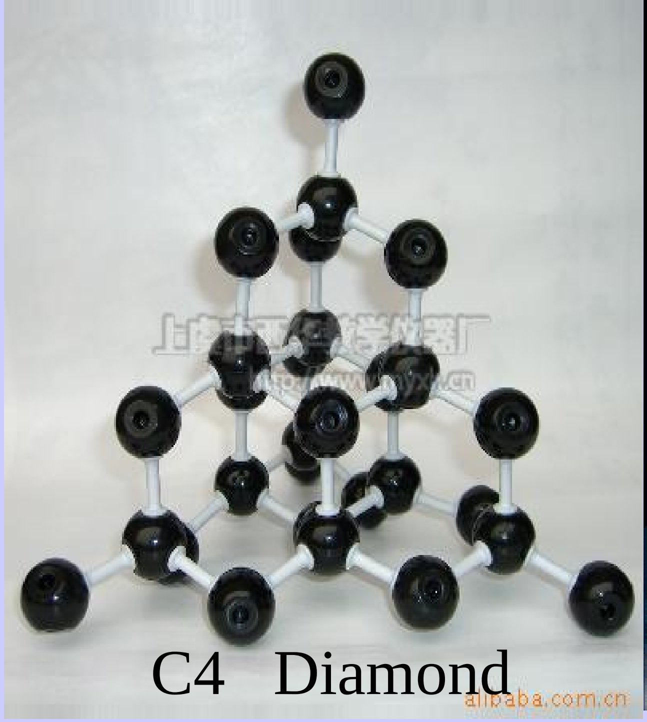

C4 Diamond

C6 Graphite

C60 Cluster

The tetrahedral symmetry in atomic nuclei,
realized at the first order
through the triaxial-octupole Y32 deformation.

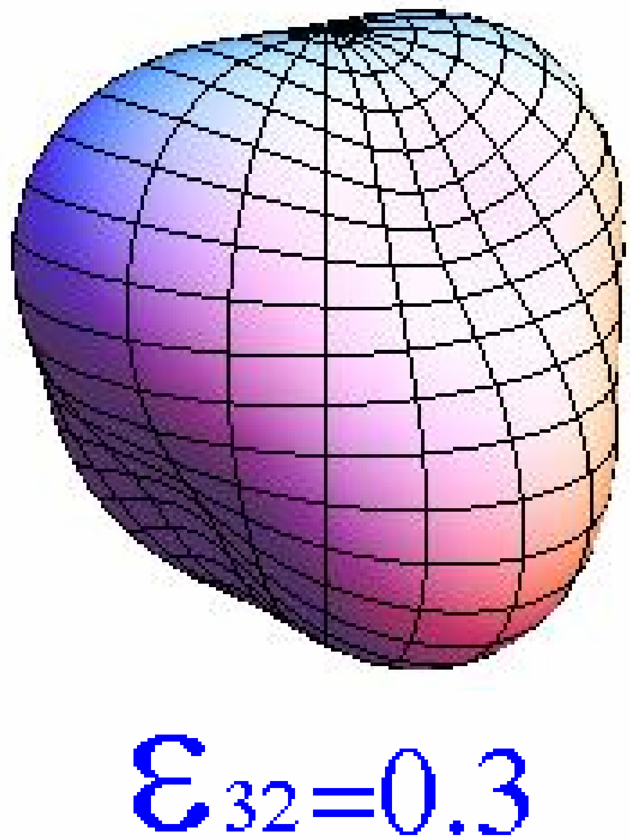

Proposed candidate of tetrahedral band negative parity band in ^{156}Gd

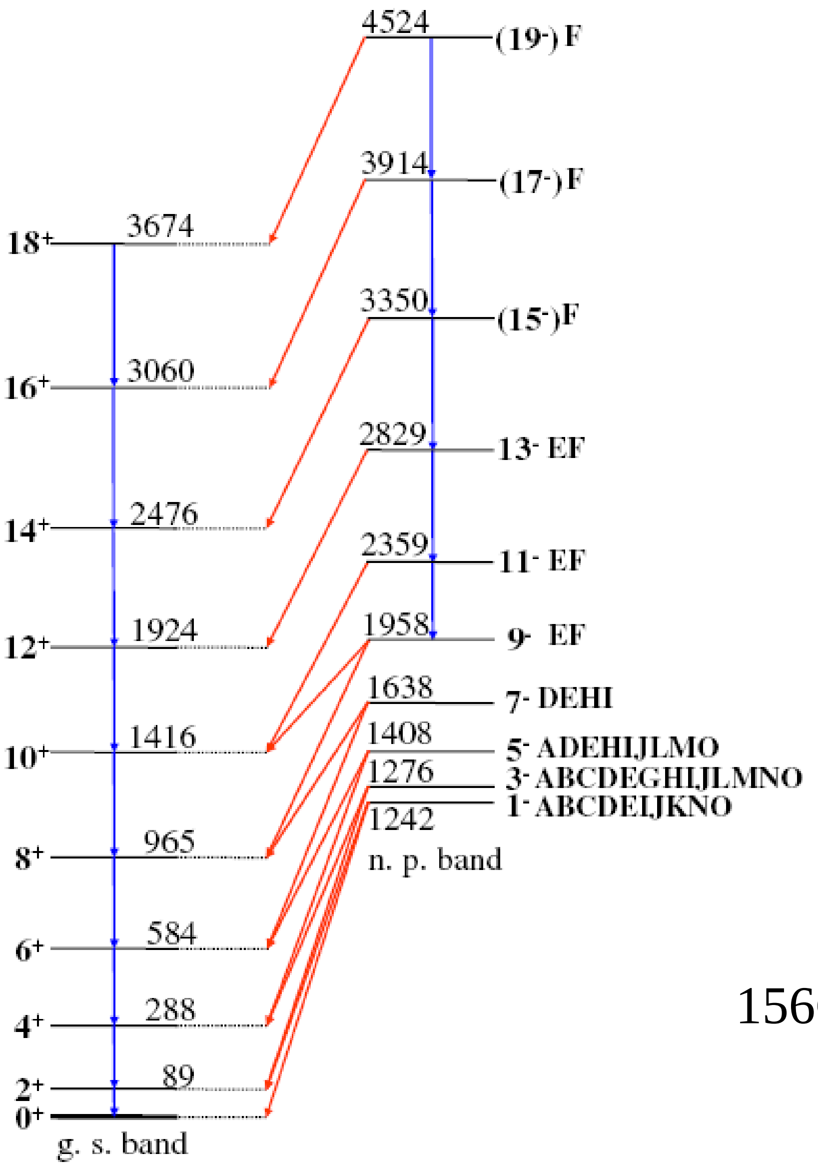

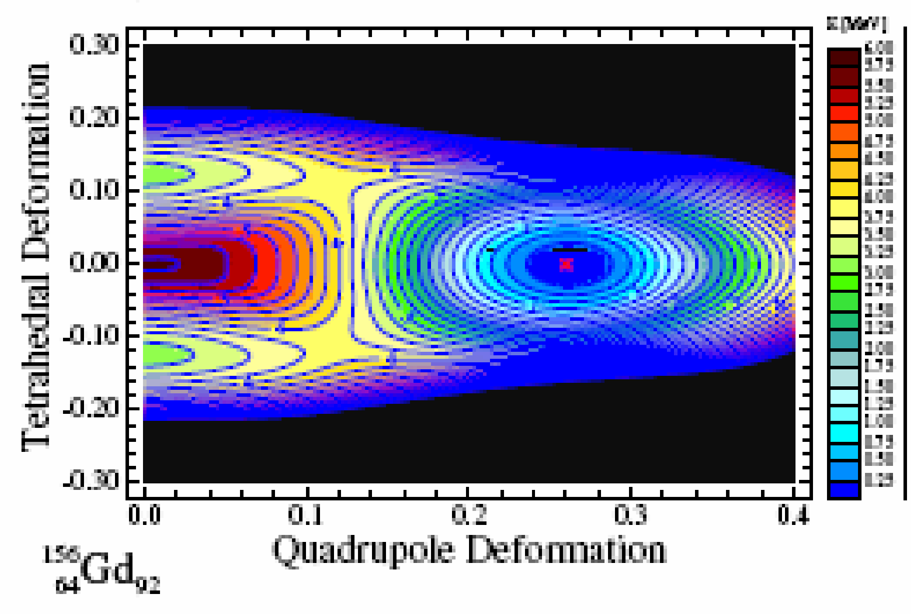

Calculation by using
standard Strutinsky method

156Gd J. Dudek et al., PRL,97,072501(2006)

Nonzero Quadrupole Moments of Candidate Tetrahedral Bands

R.A.Bark,et al., PRL 104,022501(2010)

$Q_t^{T} / Q_t^{AF} \approx 1.2 \qquad Q_t^{AF} \approx Q_t^{gb} = 6.5eb$ from band-mixing calculations

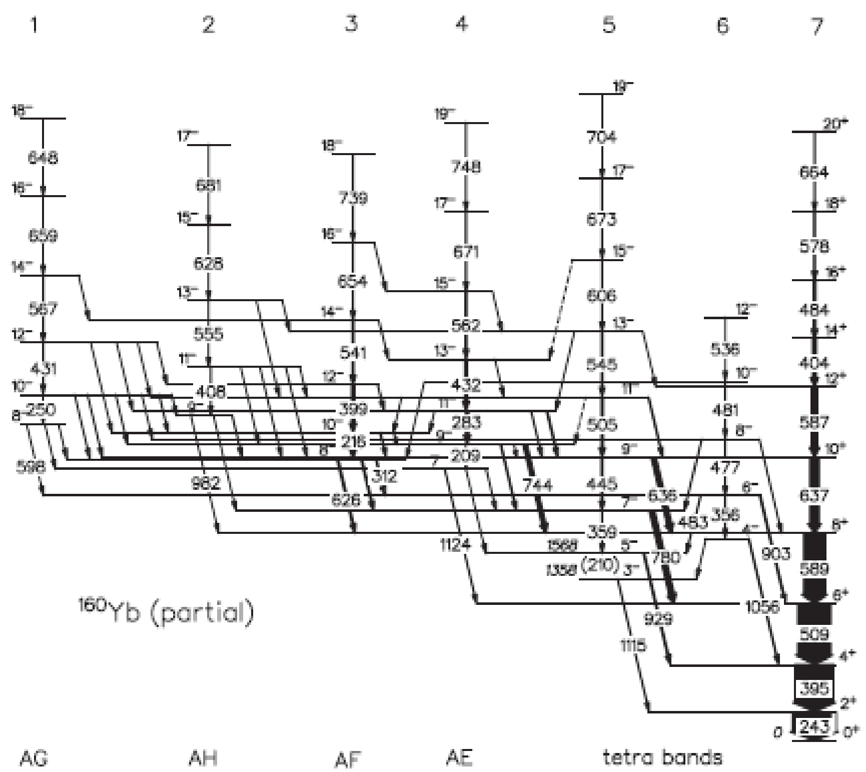

FIG. 1. Present partial scheme of ^{160}Yb. Arrow width indicates relative intensity. 210 keV transition was unobserved.

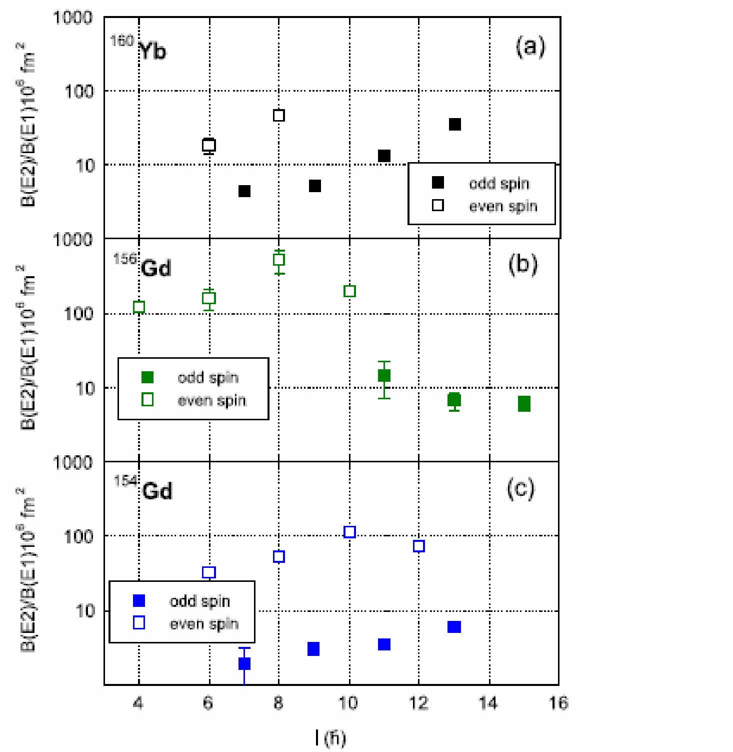

FIG. 3 (color online). $B(E2; I \to I-2)/B(E1; I \to I-1)$ (filled symbols) and $B(E2; I \to I-2)/B(E1; I \to I)$ (open symbols) values for proposed tetrahedral bands. Data for ^{156}Gd from Ref. [19].

Ultrahigh-Resolution γ-Ray Spectroscopy of 156Gd: A Test of Tetrahedral Symmetry
M. Jentschel at al. PRL 104, 222502 (2010)

Nucleus	Transition $I_i^\pi \rightarrow I_f^\pi$	E_γ (keV)	$B(E2)$ (W.u.)	$B(E1)$ (W.u. $\times 10^{-3}$)
^{154}Sm	$2_1^+ \rightarrow 0_1^+$	123.0706	157(1)[c]	
	$4_1^+ \rightarrow 2_1^+$	247.9288	245(9)[c]	
	$3_1^- \rightarrow 2_1^+$	930.37		0.80(11)[c]
	$3_1^- \rightarrow 4_1^+$	645.50		0.92(13)[c]
^{154}Gd	$2_1^+ \rightarrow 0_1^+$	123.0706	157(1)[c]	
	$4_1^+ \rightarrow 2_1^+$	247.9288	245(9)[c]	
^{156}Gd	$2_1^+ \rightarrow 0_1^+$	88.970	187(5)[b]	
	$4_1^+ \rightarrow 2_1^+$	199.219	263(5)[b]	
	$3_1^- \rightarrow 2_1^+$	1187.1631		0.98(21)[b]
	$3_1^- \rightarrow 4_1^+$	987.9440		0.77(16)[b]
	$5_1^- \rightarrow 4_1^+$	1119.9335		$0.85^{+.19}_{-.38}$[a]
	$5_1^- \rightarrow 6_1^+$	823.421		$0.64^{+.14}_{-.29}$[a]
	$5_1^- \rightarrow 3_1^-$	131.983	293^{+61}_{-134}[a]	
^{158}Gd	$2_1^+ \rightarrow 0_1^+$	79.5132	198(6)[d]	
	$4_1^+ \rightarrow 2_1^+$	181.943	289(5)[d]	
	$3_1^- \rightarrow 2_1^+$	962.122		0.33(1)[d]
	$3_1^- \rightarrow 4_1^+$	780.183		0.29(8)[d]
	$5_1^- \rightarrow 4_1^+$	915.03		$0.77^{+.23}_{-.34}$[e]
	$5_1^- \rightarrow 6_1^+$	637.469		$0.60^{+.20}_{-.27}$[e]
	$5_1^- \rightarrow 3_1^-$	134.848	355^{+103}_{-155}[e]	

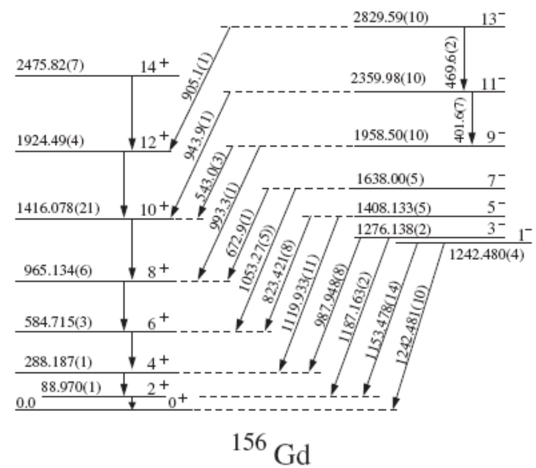

FIG. 1. Partial level scheme of ^{156}Gd, data from [9]. The ground-state band (positive parity) and the band candidate to represent tetrahedral symmetry (negative parity) are shown. Transition and level energies are given in keV.

$$5^- - state$$

$$Q_0 = 7.1^{+0.7}_{-1.6}\, b$$

This large value, comparable to the quadrupole moment of the ground state in ^{156}Gd, gives strong evidence against tetrahedral symmetry in the lowest odd-spin, negative-parity band of ^{156}Gd.

Brief description of RASM

***Symmetry broken in the intrinsic frame & restoration of Symmetry in Laboratory system :**

Reflection asymmetry → Octuple bands
Rotational asymmetry → Wobbling, Chiral, (Signature inversed) bands.

Shell model description of spectroscopy of octupole deformed nuclei:
RASM has been successful.

Nuclear pear shape is characterized by
the parity doublet rotational bands:
in even-even nuclei,
the positive parity band $I^{\pi} = 0^{+}, 2^{+}, 4^{+}, \ldots.$
and the negative parity band $I^{\pi} = 1^{-}, 3^{-}, 5^{-}, \ldots..$

There exist enhanced E1 transitions connecting the
doublet bands.

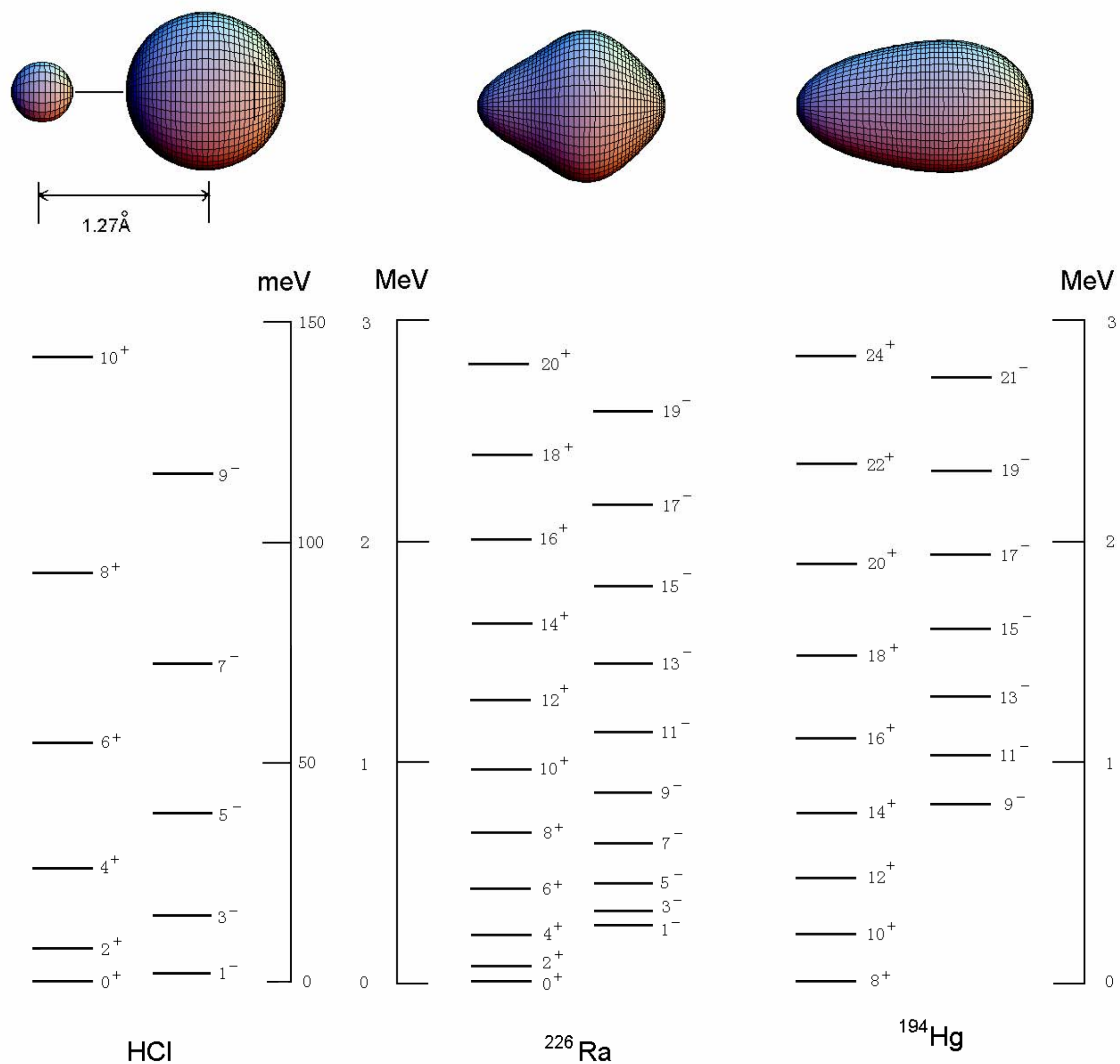
1.27Å
meV
MeV
MeV
150
100
50
0
3
2
1
0
10+
8+
6+
4+
2+
0+
9−
7−
5−
3−
1−
20+
18+
16+
14+
12+
10+
8+
6+
4+
2+
0+
19−
17−
15−
13−
11−
9−
7−
5−
3−
1−
24+
22+
20+
18+
16+
14+
12+
10+
8+
21−
19−
17−
15−
13−
11−
9−
3
2
1
0
HCl
226Ra
194Hg

RASM

(Reflection Asymmetric Shell Model)

Hamiltonian

$$H = H_0 - \sum_{\lambda=2}^{4} \frac{\chi_\lambda}{2} Q_\lambda^+ \cdot Q_\lambda - G_0 P_0^+ \cdot P_0 - G_2 P_2^+ \cdot P_2$$

$$Q_{\lambda\mu} = \sum_{\alpha,\beta} \langle \alpha | Y_{\lambda\mu} | \beta \rangle c_\alpha^+ c_\beta$$

$$P_{00}^+ = \frac{1}{2} \sum_\alpha c_\alpha^+ c_{\bar{\alpha}}^+$$

$$P_{2\mu}^+ = \frac{1}{2} \sum_{\alpha,\beta} \langle \alpha | Y_{2\mu} | \beta \rangle c_\alpha^+ c_{\bar{\beta}}^+$$

The shell model space

$$\left\{ P^{\pi} P^{I}_{MK} \middle| \Phi_{\kappa} \right\rangle \right\}$$

$$P^{\pi} = \frac{1}{2}\left(1 + \pi \hat{P}\right)$$

$$P^{I}_{MK} = \frac{2I+1}{8\pi^2} \int d\Omega D^{I}_{MK}(\Omega) \hat{R}(\Omega)$$

$$\hat{R}(\Omega) = e^{-i\alpha \hat{j}_z} e^{-i\beta \hat{j}_y} e^{-i\gamma \hat{j}_z} \quad , \quad [\hat{P}, \hat{R}(\Omega)] = 0$$

The trial wave function

$$|\Psi_{IM}^{\pi}> = \sum_{K\kappa} F_{IK\kappa}^{\pi} P^{\pi} P_{MK}^{I} |\Phi_{\kappa}>$$

$$\delta < \Psi | H | \psi > - E < \Psi | \Psi > = 0$$

The RASM eigenvalue equation

$$\sum_{K\kappa} \left\{ \left\langle \Phi_{\kappa'} \middle| H P^{\pi} P_{K'K}^{I} \middle| \Phi_{\kappa} \right\rangle - E^{I\pi} \left\langle \Phi_{\kappa'} \middle| P^{\pi} P_{K'K}^{I} \middle| \Phi_{\kappa} \right\rangle \right\} F_{K\kappa}^{I\pi} = 0$$

$$\left\langle \Psi_{IM}^{\pi} \middle| \Psi_{IM}^{\pi} \right\rangle = \sum_{KK'\kappa\kappa'} F_{K'\kappa'}^{I\pi} \left\langle \Phi_{\kappa'} \middle| P^{\pi} P_{K'K}^{I} \middle| \Phi_{\kappa} \right\rangle F_{K\kappa}^{I\pi} = 1$$

Multi-quasiparticle basic states

For even-even nuclei:

$$\left\{\hat{P}^{I\pi}_{MK}\left|0\right\rangle, \hat{P}^{I\pi}_{MK}\alpha^+_\nu\alpha^+_\nu\left|0\right\rangle, \hat{P}^{I\pi}_{MK}\alpha^+_\pi\alpha^+_\pi\left|0\right\rangle, \hat{P}^{I\pi}_{MK}\alpha^+_\nu\alpha^+_\nu\alpha^+_\pi\alpha^+_\pi\left|0\right\rangle, \ldots\right\}$$

For odd-odd nuclei:

$$\left\{\hat{P}^{I\pi}_{MK}\alpha^+_\nu\alpha^+_\pi\left|0\right\rangle, \hat{P}^{I\pi}_{MK}\alpha^+_\nu\alpha^+_\nu\alpha^+_\nu\alpha^+_\pi\left|0\right\rangle, \hat{P}^{I\pi}_{MK}\alpha^+_\nu\alpha^+_\pi\alpha^+_\pi\alpha^+_\pi\left|0\right\rangle, \hat{P}^{I\pi}_{MK}\alpha^+_\nu\alpha^+_\nu\alpha^+_\nu\alpha^+_\pi\alpha^+_\pi\alpha^+_\pi\left|0\right\rangle, \ldots\right\}$$

For odd-neutron nuclei:

$$\left\{\hat{P}^{I\pi}_{MK}\alpha^+_\nu\left|0\right\rangle, \hat{P}^{I\pi}_{MK}\alpha^+_\nu\alpha^+_\pi\alpha^+_\pi\left|0\right\rangle, \hat{P}^{I\pi}_{MK}\alpha^+_\nu\alpha^+_\nu\alpha^+_\nu\alpha^+_\pi\alpha^+_\pi\left|0\right\rangle, \ldots\right\}$$

For odd-proton nuclei:

$$\left\{\hat{P}^{I\pi}_{MK}\alpha^+_\pi\left|0\right\rangle, \hat{P}^{I\pi}_{MK}\alpha^+_\nu\alpha^+_\nu\alpha^+_\pi\left|0\right\rangle, \hat{P}^{I\pi}_{MK}\alpha^+_\nu\alpha^+_\nu\alpha^+_\pi\alpha^+_\pi\alpha^+_\pi\left|0\right\rangle, \ldots\right\}$$

EXP. ° **negative parity**

● **positive parity**

Theor. ——

N=4,5,6 for protons
N=5,6,7 for neutrons

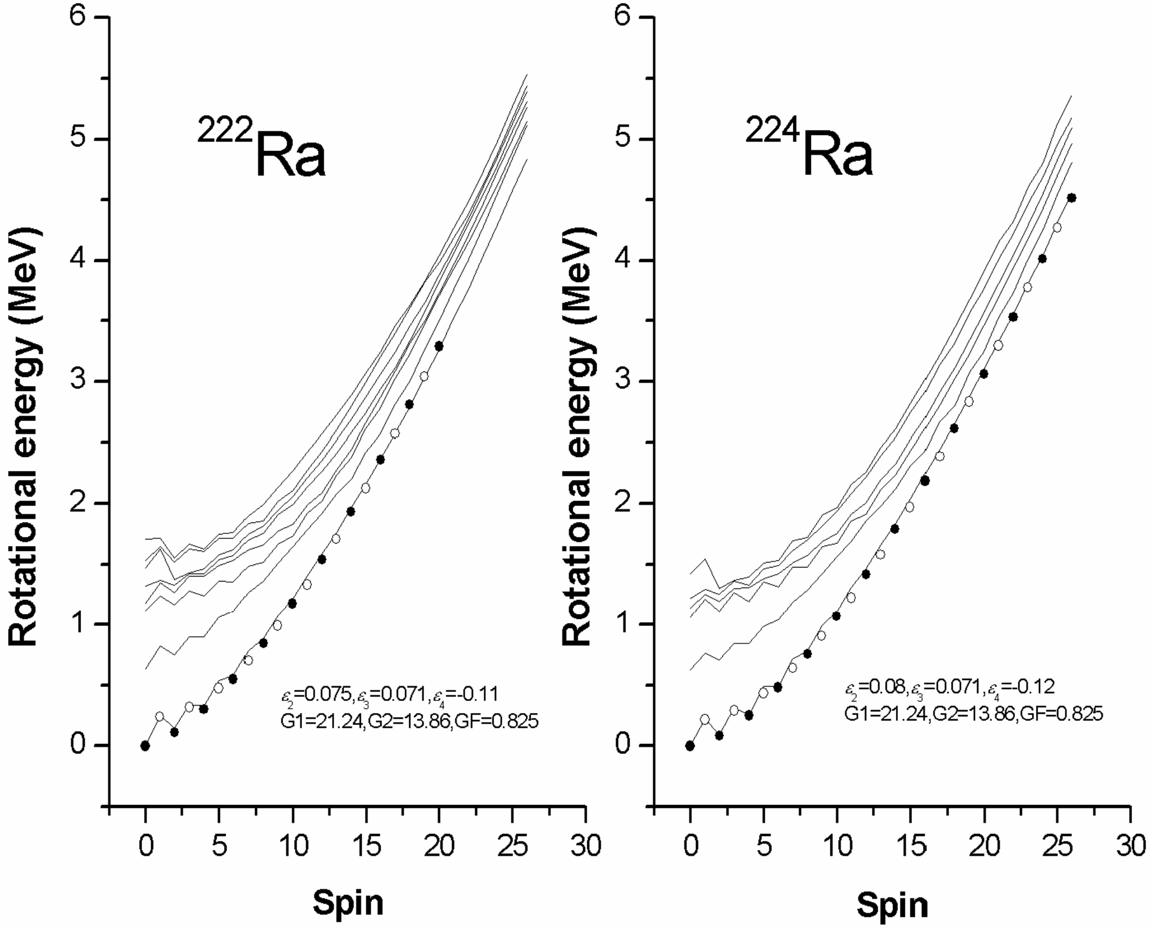

Y.S. Chen and Z.C. Gao Phys. Rev. C63, 014314 (2001)

3. Tetrahedral nuclear spectroscopy

Nature of low-lying 2^- bands in transfermium nuclei

N = 150 2^- band heads

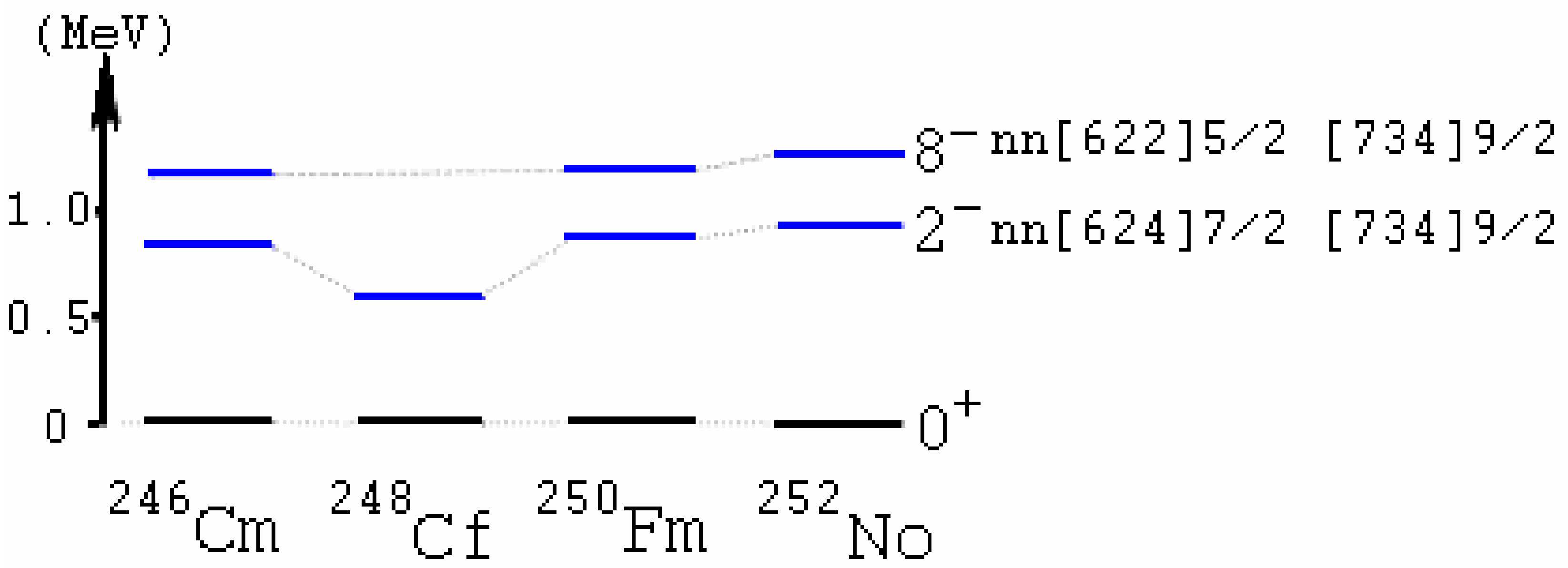

Low lying negative parity bands with $I^{\pi} = 2^{-}, 3^{-}, 4^{-}, \ldots$ interpreted as the obscured tetrahedral bands by RASM

Nuclei with shape of $Y_{20} + Y_{32}$

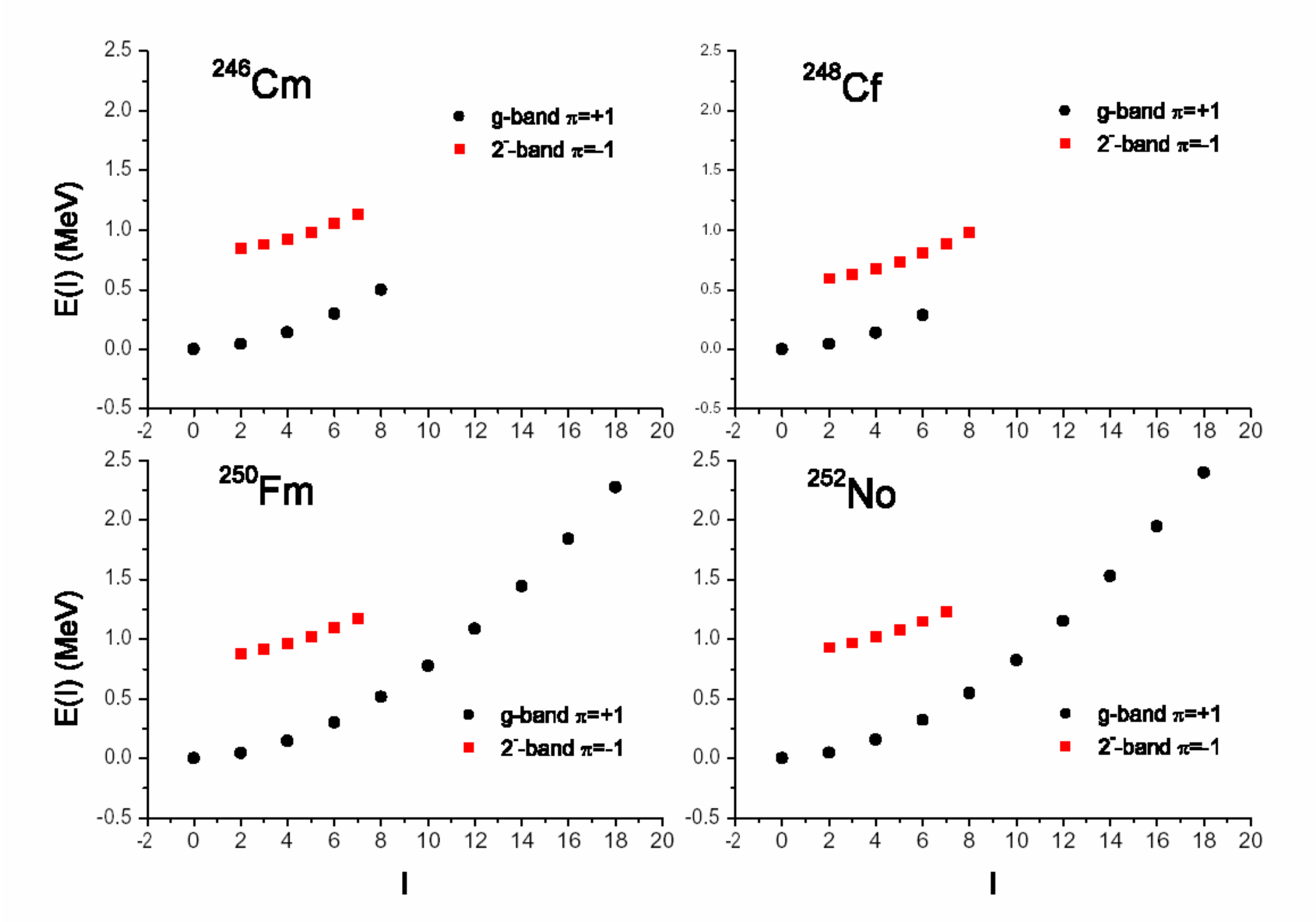

$Y_{20+}Y_{32}$

Symmetry: $\hat{P}e^{i\pi\hat{J}_z/2}$

K, p : $pe^{i\pi K/2}=1$

Namely , $K^p = 0^+, \pm 2^-, \pm 4^+, \ldots$

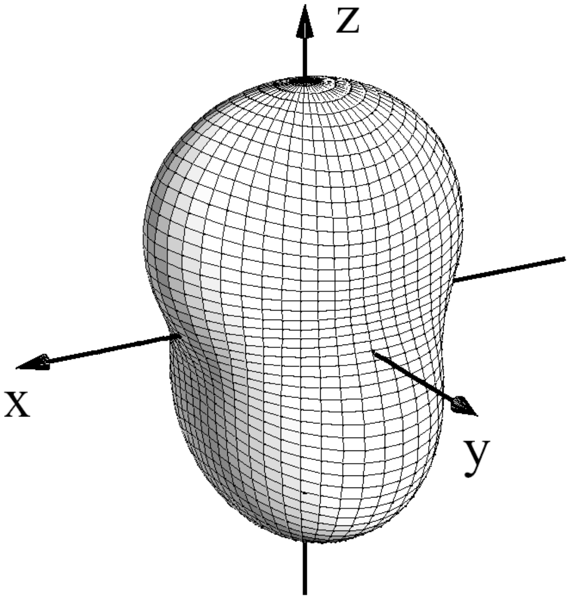

$K = 0$	$0^+,\ 2^+, 4^+,\ldots$
$K = 2$	$2^-, 3^-, 4^-,\ldots$
$K = 4$	$4^+,\ 5^+, 6^+,\ldots$

S_y

$K = 0$	$0^+, 1^-, 2^+, 3^-,\ldots[p(-1)^I=1]$
$K > 0$	$K^\pm, (K+1)^\pm, (K+2)^\pm,\ldots$

Non-axial octupole bands in N=150 isotones

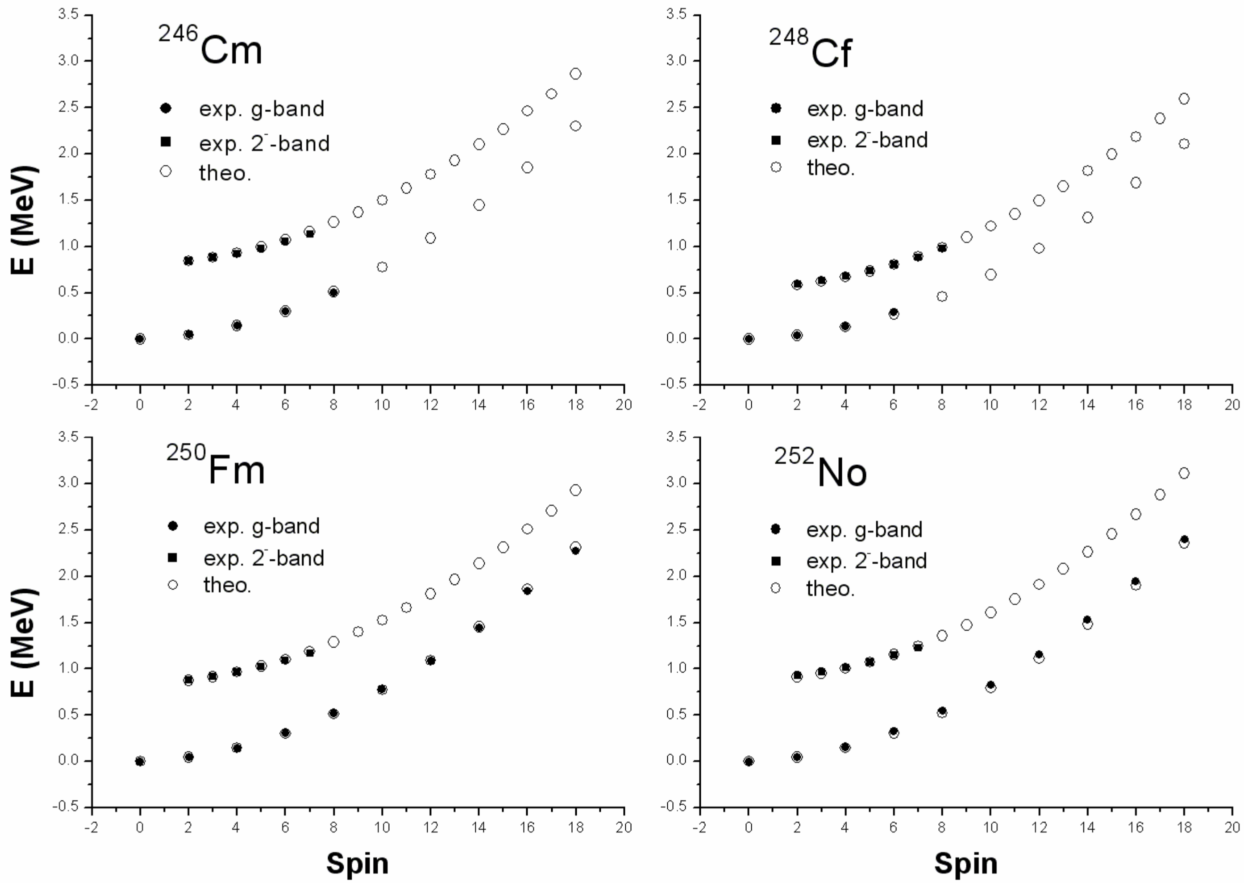

$$\varepsilon_2 \approx 0.235, \varepsilon_{32} \approx 0.11$$

Y.S. Chen, Yang Sun, Zao-Chun Gao , Phys. Rev. C 77 , 061305 (R) (2008)

Tetrahedral states

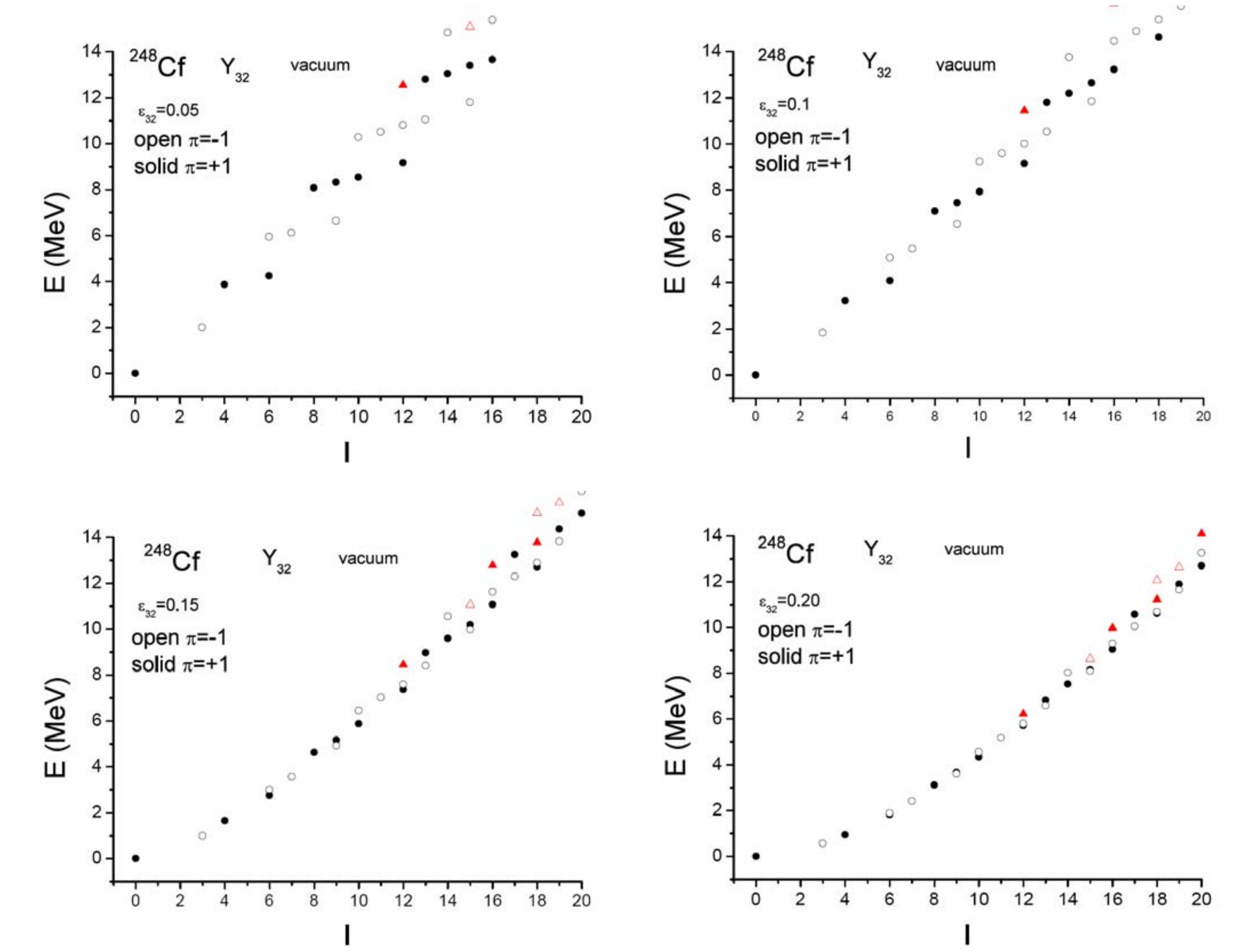

Very
low-lying State

3^-

Missing
Low-lying State

2^+

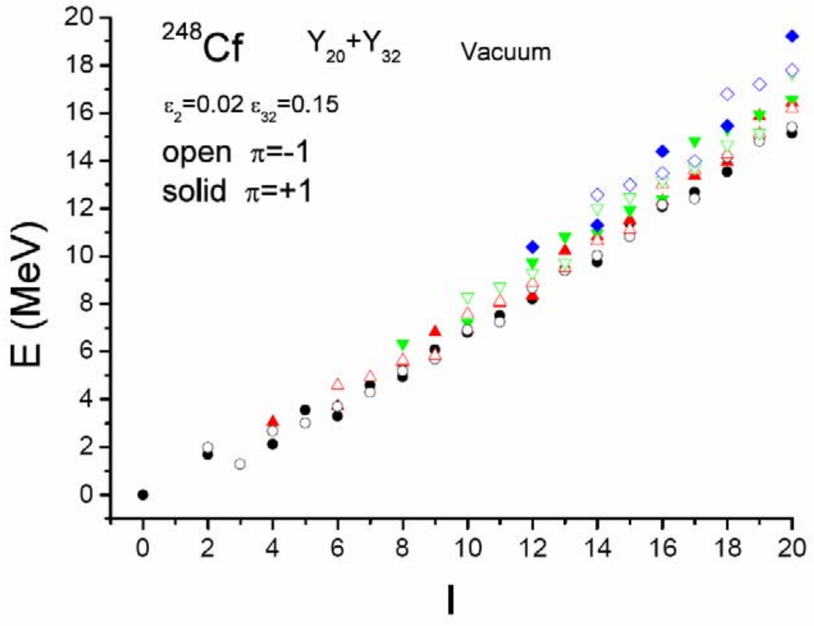

More realistic case may be tedrahedral shape with very small quadrupole deformation:

3^- *state*

is lower than

2^- *and* 2^+

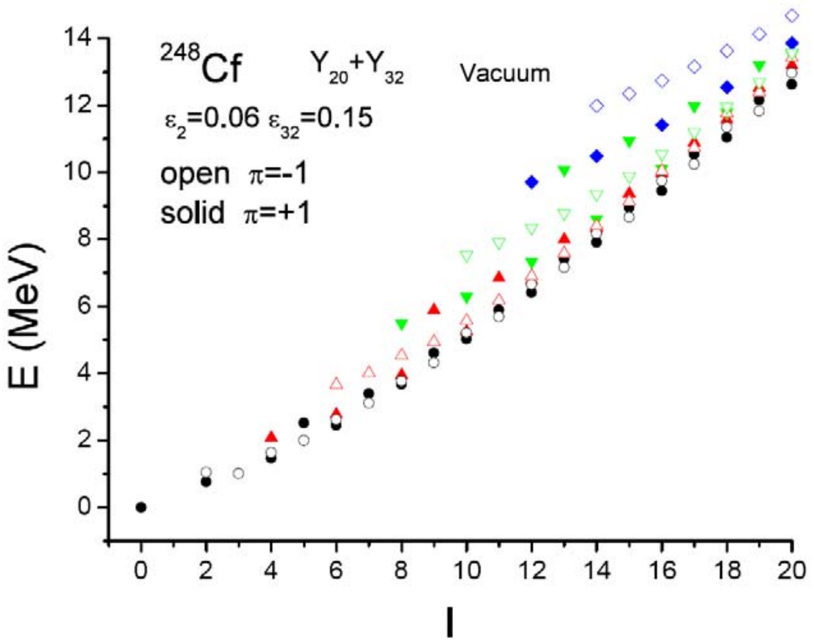

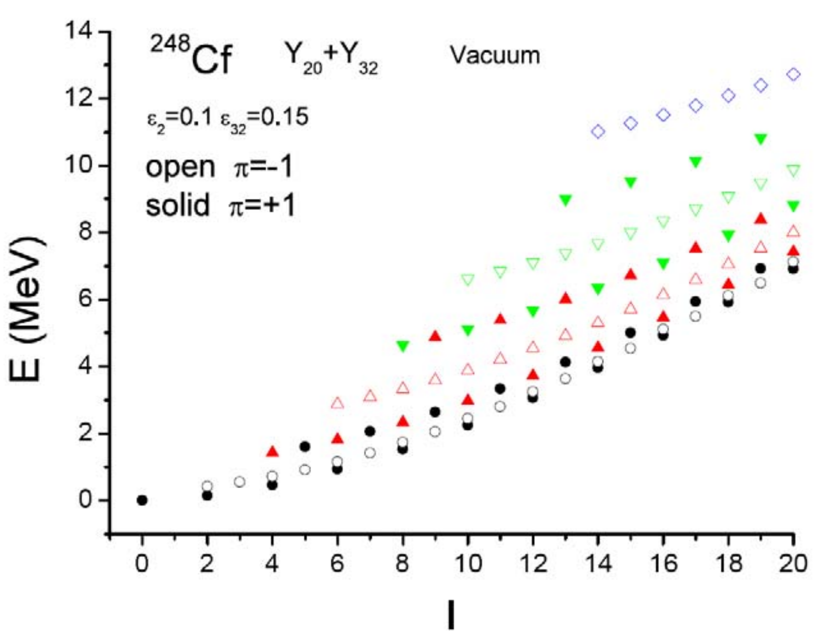

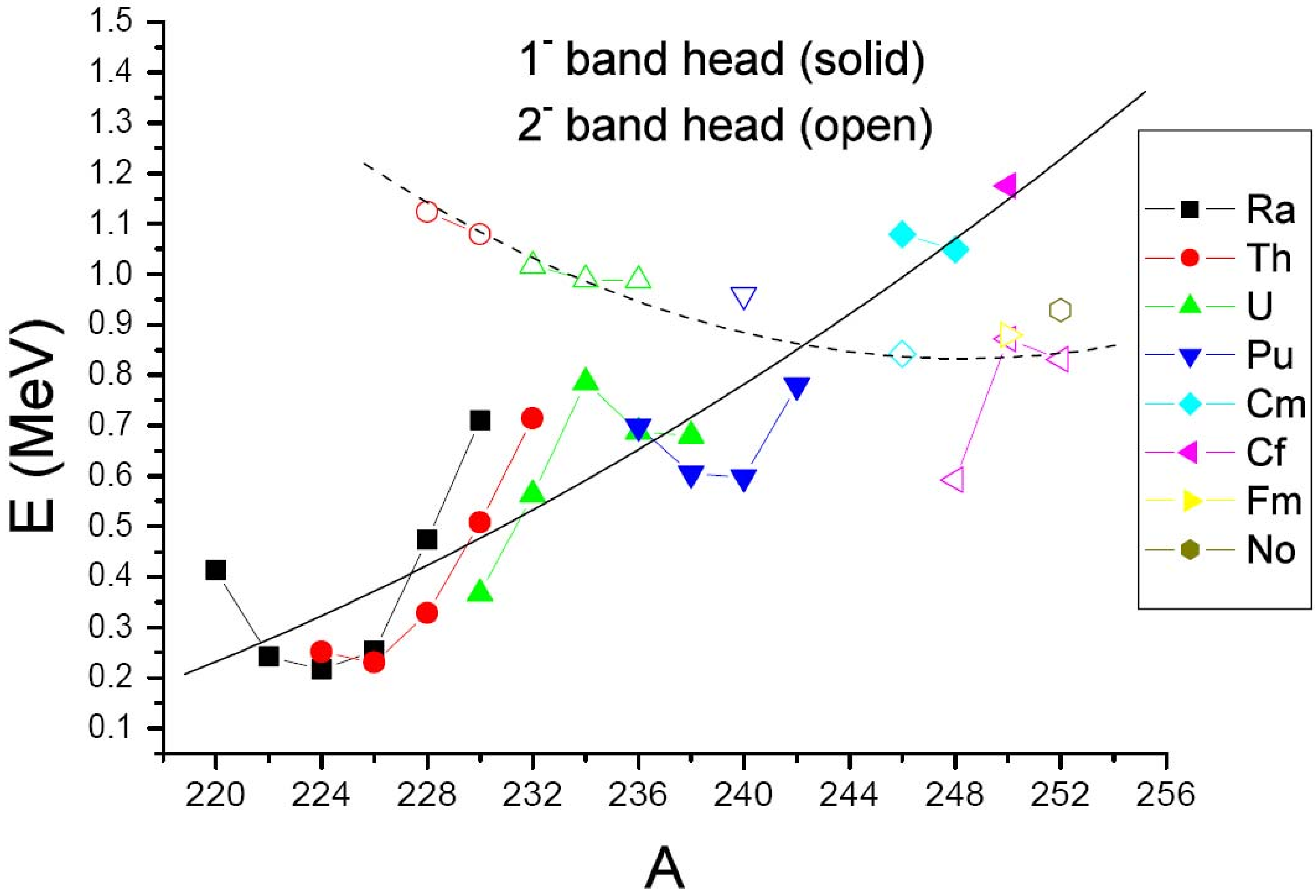

Y.S. Chen, Yang Sun, Zao-Chun Gao , Phys. Rev. C 77 , 061305 (R) (2008)

Tetrahedral symmetry in SHE

Projected Energy Surface (PES) based on RASM

$$E^{I\pi} = \frac{<\Psi_{I\pi} | \hat{H} | \Psi_{I\pi}>}{<\Psi_{I\pi} | \Psi_{I\pi}>}$$

$$|\Psi^{\pi}_{IM}> = \sum_{K\kappa} f^{\pi}_{IK\kappa} P^{\pi} P^{I}_{MK} |\Phi_{\kappa}>$$

Single particle diagram

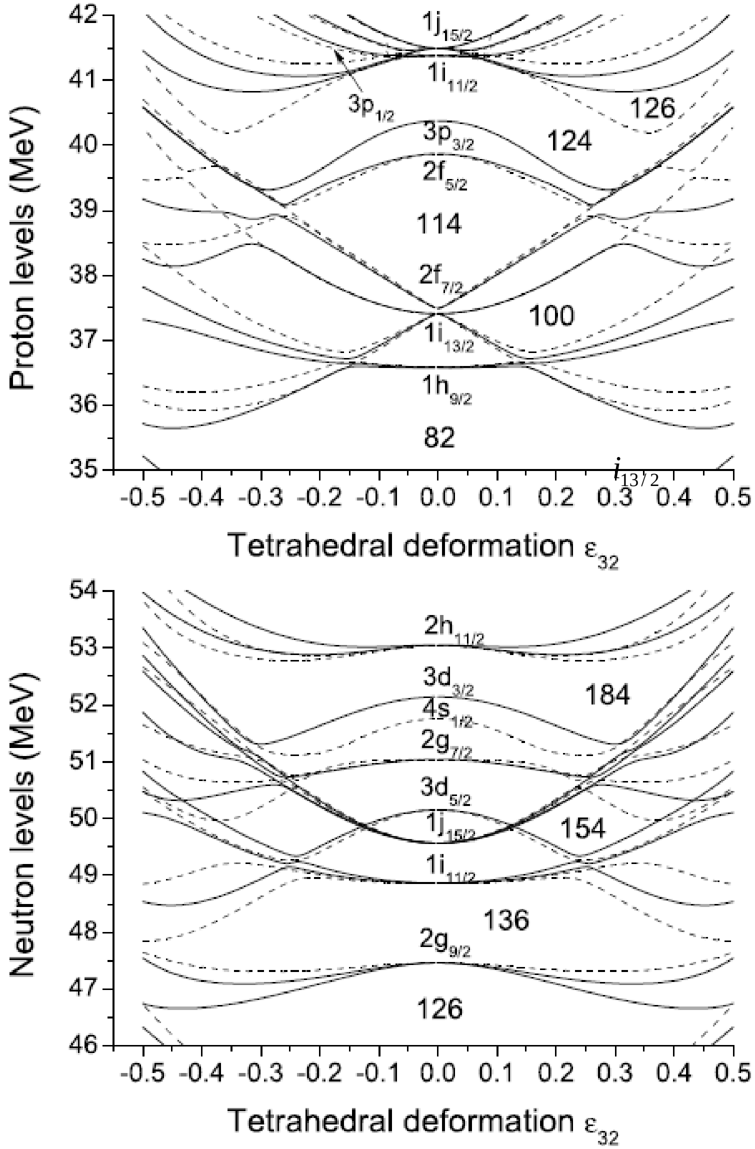

Octupole coupling

$$i_{13/2} \leftrightarrow f_{7/2} \qquad i_{11/2} \leftrightarrow f_{5/2}$$

$$\Delta j = \Delta l = 3$$

$$j_{15/2} \leftrightarrow g_{9/2} \qquad h_{11/2} \leftrightarrow d_{5/2}$$

Shell energy for (Z=126,N=184)

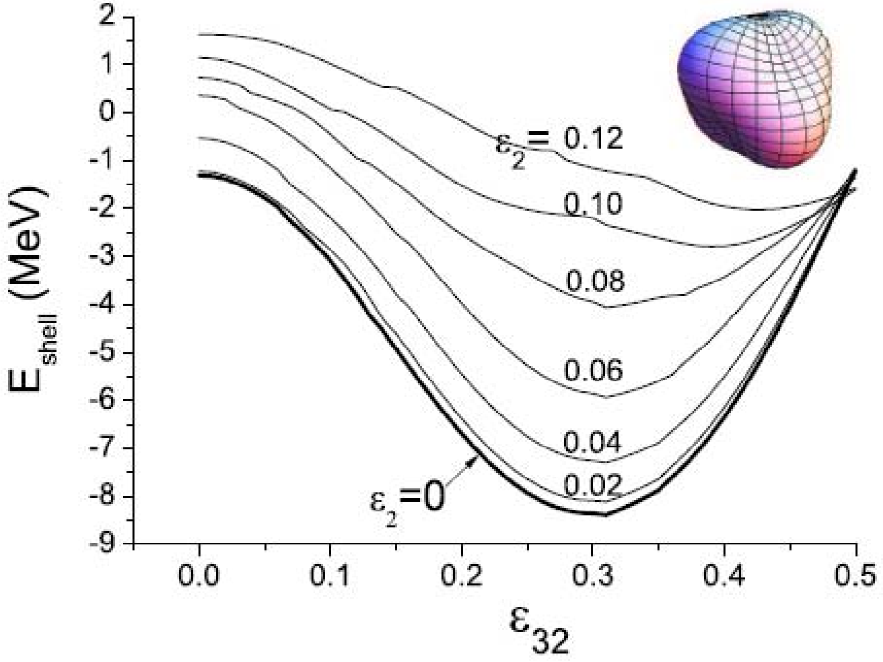

Well defined tetrahedral minimum for (Z=126,N=184)

Projected energy surfaces

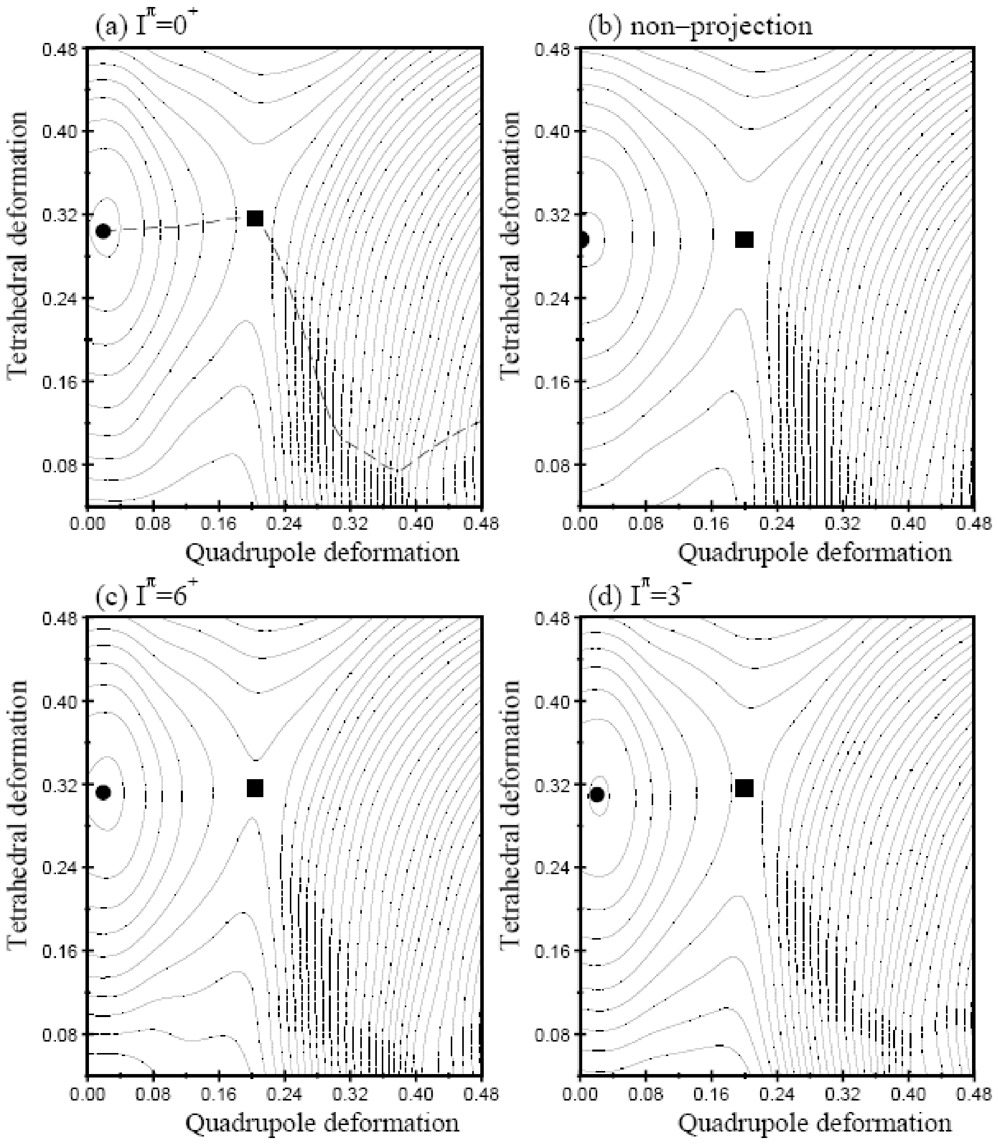

Fission Barriers

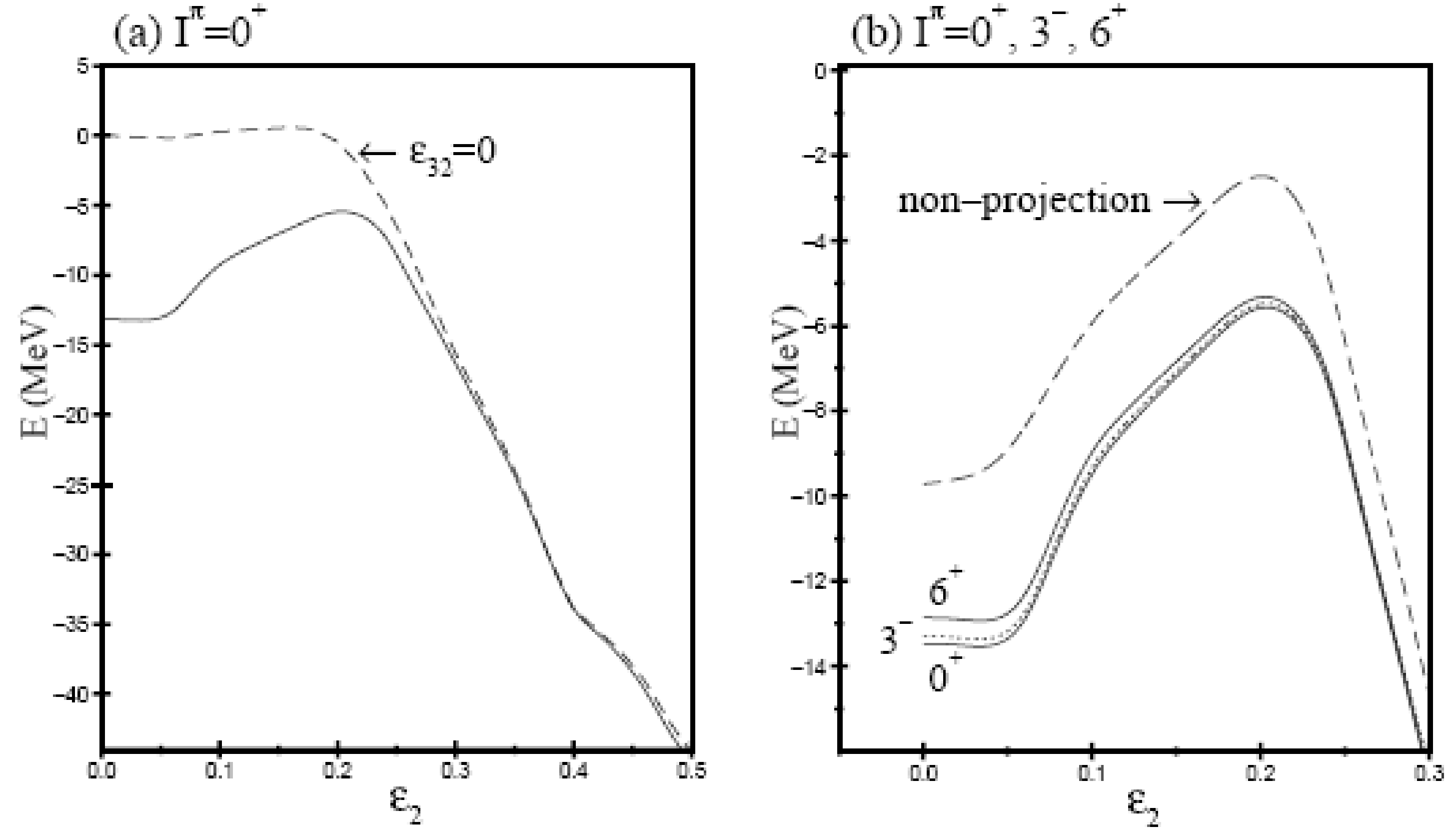

Vol. 40 (2009) ACTA PHYSICA POLONICA B No 3

NEW NUCLEAR STABILITY ISLANDS OF OCTAHEDRAL AND TETRAHEDRAL SHAPES*

K. Mazurek[a], J. Dudek[b], A. Góźdź[c], D. Curien[b]
M. Kmiecik[a], A. Maj[a]

[a]The Niewodniczański Institute of Nuclear Physics PAN
Radzikowskiego 152, 31-342 Kraków, Poland
[b]Institut Pluridisciplinaire Hubert Curien, IN2P3-CNRS
and
Université Louis Pasteur, 67037 Strasbourg Cedex 2, France
[c]Zakład Fizyki Matematycznej, Uniwersytet Marii Curie-Skłodowskiej
Pl. Marii Curie-Skłodowskiej 1, 20-031 Lublin, Poland

$\triangle$ Esh=Esh(Q) –Esh(T)

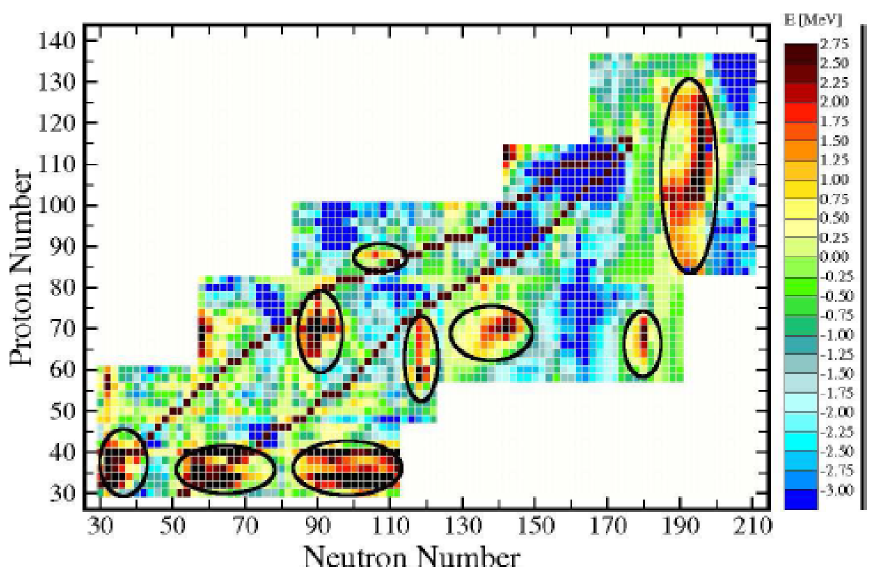

Fig. 3. Differences of the shell-energies as discussed in the text.

Shell energy minimized
with respect to
Quadrupole and
hexadecapole
Minus
Shell energy minimized
with respect to
tetrahedral and octahedral

Microscopic-Macroscopic method
Woods-Saxon potential

K. Mazurek et al., Acta Physica Pol. B 40, 731 (2009).

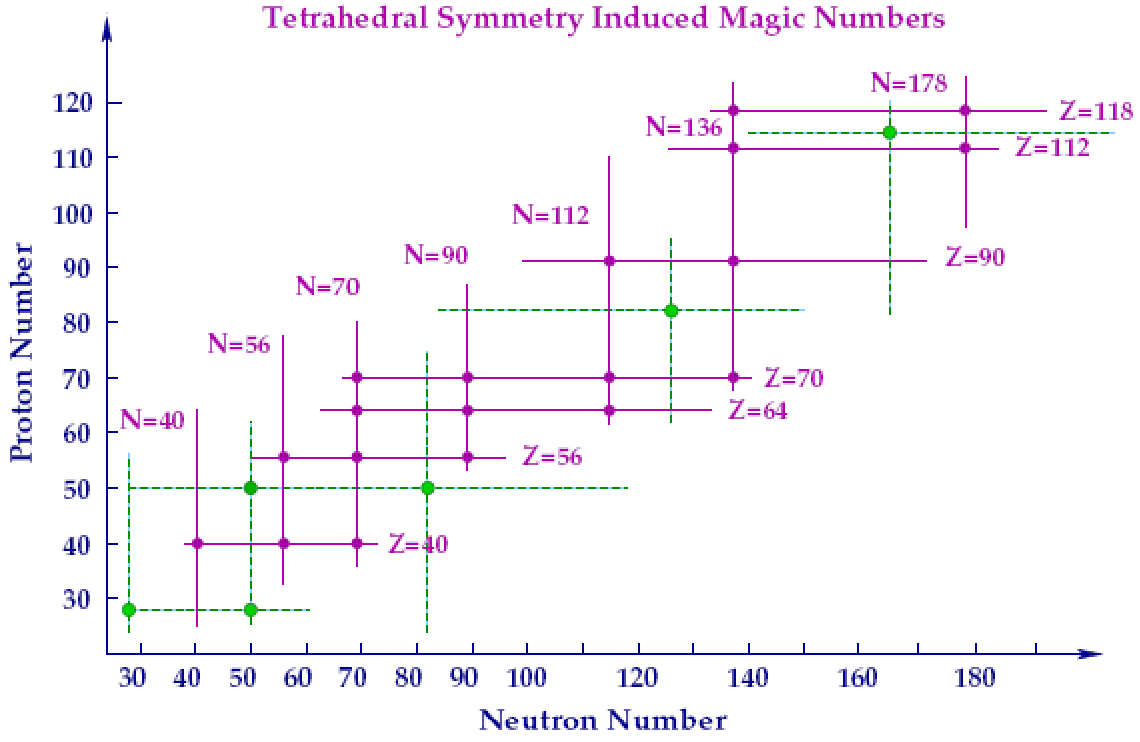

Fig. 1. Each mean-field symmetry generates its 'magic' numbers corresponding to an increased nuclear stability. Points connected with the dashed lines correspond to the spherical-symmetry well-known magic numbers (including the super-heavy nuclei). The points connected with full lines represent the result of the systematic mean-field calculations for the tetrahedral symmetry as discussed in the text.

International Journal of Modern Physics E
Vol. 20, No. 2 (2011) 514–519

World Scientific
www.worldscientific.com

TEST OF TETRAHEDRAL SYMMETRY FOR
HEAVY AND SUPERHEAVY NUCLEI

P. JACHIMOWICZ and P. ROZMEJ
Institute of Physics, University of Zielona Góra,
Szafrana 4a, 65516 Zielona Góra, Poland

M. KOWAL, J. SKALSKI and A. SOBICZEWSKI
Soltan Institute for Nuclear Studies, Hoża 69, PL-00-681 Warsaw, Poland
mkowal@fuw.edu.pl

Microscopic -Macroscopic method

Micro-part: Woods Saxon potential
Macro- part :Yukawa plus exponential model

Multi-D, 12 dimensional manifold of shapes
β_{20}, β_{22}, β_{30}, β_{32}, β_{40}, β_{42}, β_{44}, β_{50}, β_{52}, β_{60}, β_{70}, β_{80}

Conditional (β20=0) tetrahedral minima

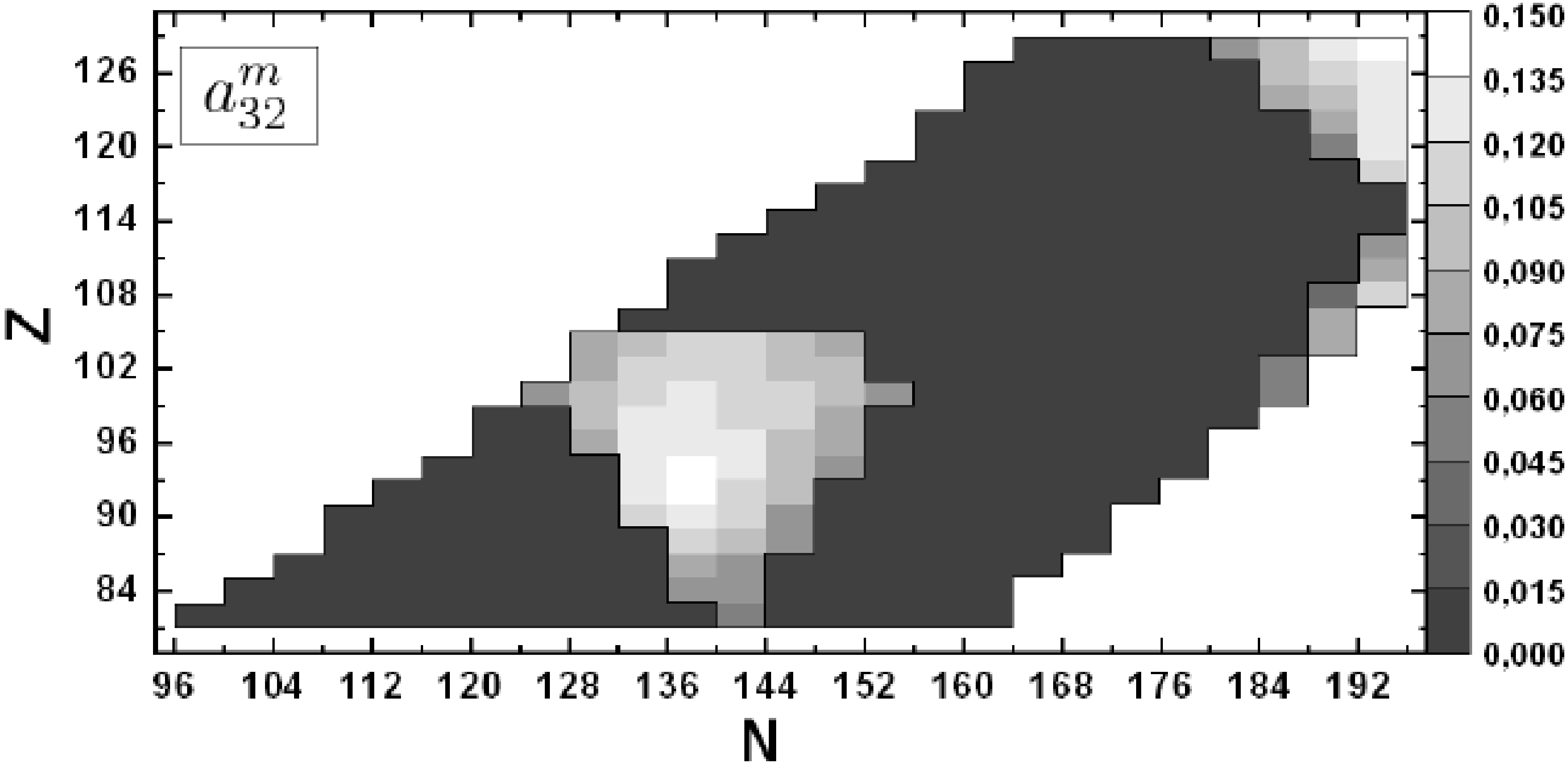

(Minimization over all the remaining 10 variables)

P. Jachimowicz et al., Int. J. Mod. Phys. E 20, 514 (2011).

Energy Surfaces
multi-D Micro.-Macro.

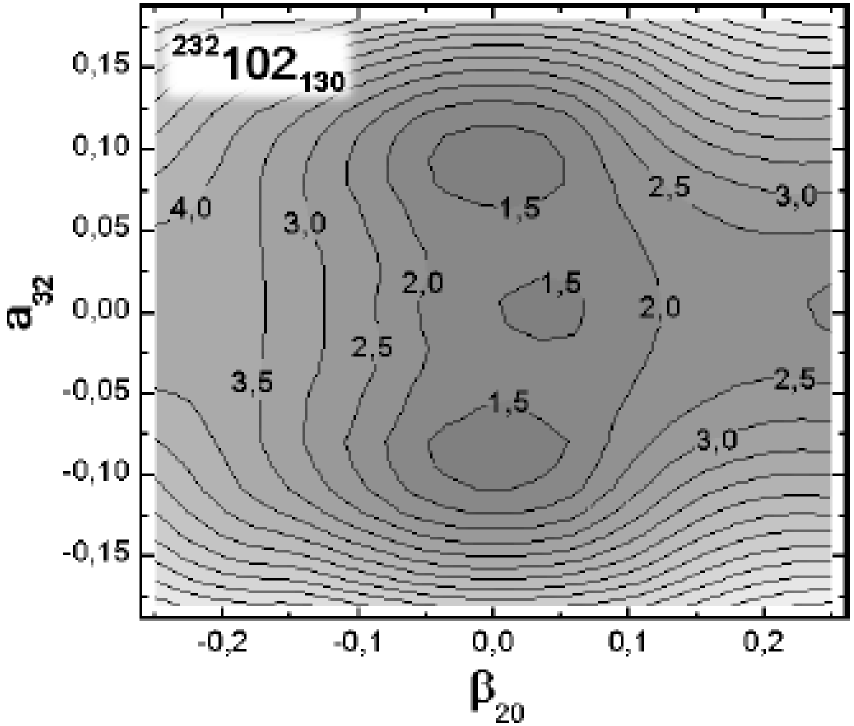

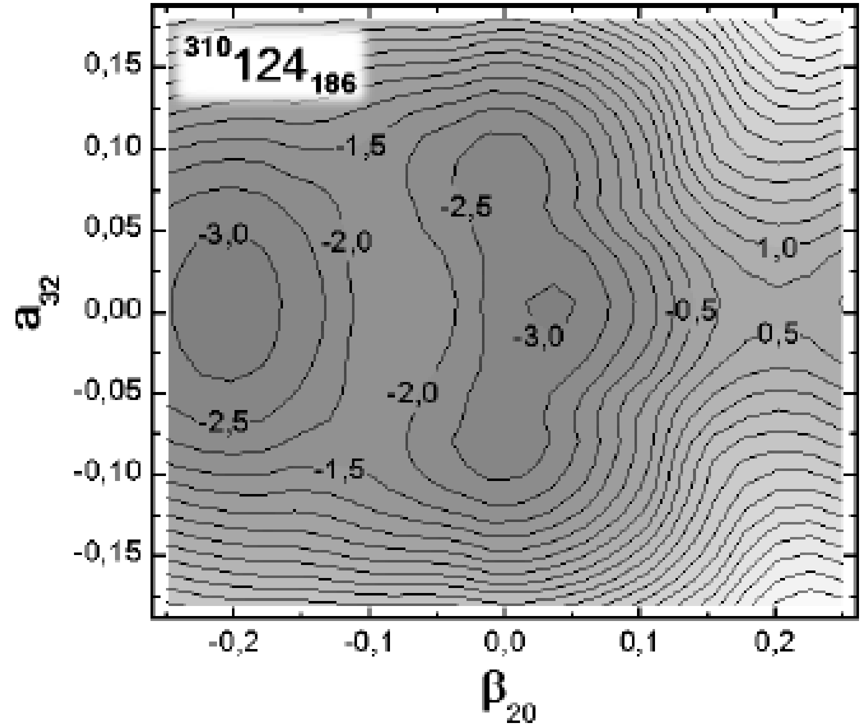

Fig. 4. Energy landscape in the (β_{20}, a_{32}) plane (with $\gamma = 0^{\circ}$) obtained after the minimization over: $\beta_{30}, \beta_{40}, \beta_{42}, \beta_{44}, \beta_{50}, \beta_{52}, \beta_{60}, \beta_{70}, \beta_{80}$, for the nuclei $^{310}124, ^{232}102$.

P. Jachimowicz et al., Int. J. Mod. Phys. E 20, 514 (2011).

Conclusions in muti-D Micro.-Macro. Calculation

P. Jachimowicz et al., Int. J. Mod. Phys. E 20, 514 (2011).

1) Have not found global tetrahedral minima.

2) Can not confirm the existence of tetrahedral magic numbers predicted in the superheavy region by **K. Mazurek et al., Acta Physica Pol. B 40, 731 (2009).**

Remarks

1. Tetrahedral symmetry-driven Shell effect is strong in the SHE region.
   No contradiction between PES, muti-D micro-macro method and normal micro-macro method.

2. Contradiction between muti-D and normal Micro.-Macro. methods may be caused by the different modelings of macro.-part.

3. Only for 0.5MeV, the muti-D micro.-macro. leads to a conclusion against the normal Micro.-Macro. calculation.

4. The beyond mean field effects may remove the bifurcations between Jachimowicz(2011) and Mazurek(2009).

Suggestion for RMF calculation with tetrahedral degree of freedom

Worth to carry out RMF calculation for tetrahedral magic superheavy nuclei around z=118-126, N=182-186

Single particle diagram for tetrahedral shape in SHE region to see tetrahedral magic gaps.

Shell energy and Total Energy surfaces calculations.

Compared to the most recent calculations of different models.

Thank you